# Breaking Waves Effects on Scatterometer and Radiometer Signatures of the Ocean


William J. Plant
Applied Physics Laboratory
University of Washington
Seattle, WA 98105, USA
plant@apl.washington.edu

Vladimir Irisov
ZelTech/NOAA
Boulder, CO 80305, USA
Vladimir.Irisov@noaa.gov



*Abstract*— **Active and passive microwave signatures of the ocean depend on the ocean wave spectrum alone if bound and breaking waves are neglected. History has not been kind to attempts to explain both radiometer brightness temperatures ($T_b$) and the normalized radar cross section ($\sigma_o$) of the sea using the same ocean wave spectrum. In this paper, we show that bound and breaking waves can be included in previous models of radiometer and scatterometer microwave signatures of the ocean to allow a single wave spectrum to explain both $T_b$ and $\sigma_o$. Bound waves are the roughness produced by gently breaking, or crumpling, waves that travel near the speed of the parent wave while breaking waves are more violent. Breaking wave and foam modeling both build on the function $\Lambda(c_b)$ introduced by Phillips, which describes the average length of breaking wave fronts on the ocean per unit area as a function of breaker velocity, $c_b$. We model a form for $\Lambda(c_b)$, particularly around its peak, based on experimental shapes, the speed of the interference pattern produced by the wave spectrum, and the balance between wind input and dissipation described by the spectrum and $\Lambda(c_b)$. Thus the wave spectrum completely determines $\Lambda(c_b)$. We show that the result of including bound and breaking waves in radiometer and scatterometer models of oceanic signatures is a much closer fit to data using a single spectrum.**



**Keywords—wave breaking, microwave emission and scattering from the sea surface**


## I. INTRODUCTION

Historically, models of microwave signatures of the sea surface have assumed that all waves on the surface are freely propagating wind-generated waves that might be modulated by longer waves [1]. Furthermore, the signatures of active microwave systems (radars and scatterometers) have been modeled independently of those of passive systems (radiometers). This led to the impossible situation that brightness temperatures, $T_b$, of radiometers were explained by surface wave spectra that were very different from those used to model normalized radar cross sections, $\sigma_o$, from scatterometers.

Here we outline the development of a joint active/passive microwave signature model of the sea surface that uses a single surface wave spectrum. We develop a form for Phillips' Lambda function, $\Lambda(\mathbf{c_b})$, directly from this spectrum [2]. We use this form to build a model of violently breaking waves and use the bound waves of Plant to model more gently breaking waves [3]. In this manner, we obtain much better fits to $\sigma_o$ data at high incidence angles and explain $T_b$ based on the roughness and foam produced by the breaking waves.

## II. RELATING PHILLIPS' Λ-FUNCTION TO THE OCEAN WAVE SPECTRUM

In 1985, Phillips proposed a quantity he called $\Lambda(\mathbf{c_b})$ to describe various statistical properties of breaking waves [2]. $\Lambda(\mathbf{c_b})$ itself describes the average crest length per unit area of breaking regions traveling at the velocity $\mathbf{c_b}$. Its first moment yields the rate at which breaking waves will be observed at a point in space. When converted to a function of wavenumber, its first moment gives the fractional area covered by whitecaps at a given time assuming a constant lifetime of foam. Its fifth moment is proportional to the energy dissipated by breaking waves. Subsequent experiments established that $\Lambda(c_b)$ peaks at speeds characteristic of rather short waves on the surface. Plant recently related the speed at which this peak occurs, the speed of surface waves most likely to break, to the phase speed at the peak of the wave spectrum through the interference pattern formed by the nearly dominant waves on the surface [4]. We utilize these observations to construct a form for $\Lambda(\mathbf{c_b})$ to use in our modeling of the microwave signatures of breaking waves.

We use three ideas to relate the form of $\Lambda(c_b)$ to the surface wave spectrum.

1. The shape of $\Lambda(c_b)$ is based on many experiments conducted over the last several years.
2. The location of the peak of $\Lambda(c_b)$ is related to the phase speed of the wave at the maximum of the wavenumber spectrum, $c_o$, as obtained by Plant [4]
3. The amplitude of $\Lambda(c_b)$ is obtained by relating the wind input to the wave energy to the energy dissipated by wave breaking.

If we let

$$\Lambda(\mathbf{c_b}) = \Lambda(c_b)D(\phi)/c_b$$

where

$$D(\phi) = 0.35\,\mathrm{sech}^2(0.7\phi)$$

then a close fit to the data can be obtained by letting

$$\Lambda(c_b) = A\,x^2/(4 + x^{10})$$

where

$$x = c_b/c_o.$$

The relationship between $c_b$ and $c_o$ was determined by Plant [4]. His data can be fit by the following form:

$$c_o = 0.22 + 0.39c_p - 0.008c_p^2$$

Finally, we can determine the constant A by relating wind input to dissipation:

$$\frac{b}{g^2}\int c_b^5\,\Lambda(c_b)\,dc_b = R\int \beta\psi(\mathbf{k})d\mathbf{k}$$

Where b is an empirical constant characterizing the fraction of wind energy lost due to breaking (Phillips, 1985), g is the acceleration of gravity, R is the ratio of wind input to dissipation determined by Banner and Morrison [5]. Based on the literature, a viable value for b is $5\cdot10^{-4}$.

Figure 1 shows this form for the DBP spectrum of Plant (2002) at a wind speed of 10 m/s and a fetch of 100 km [6].

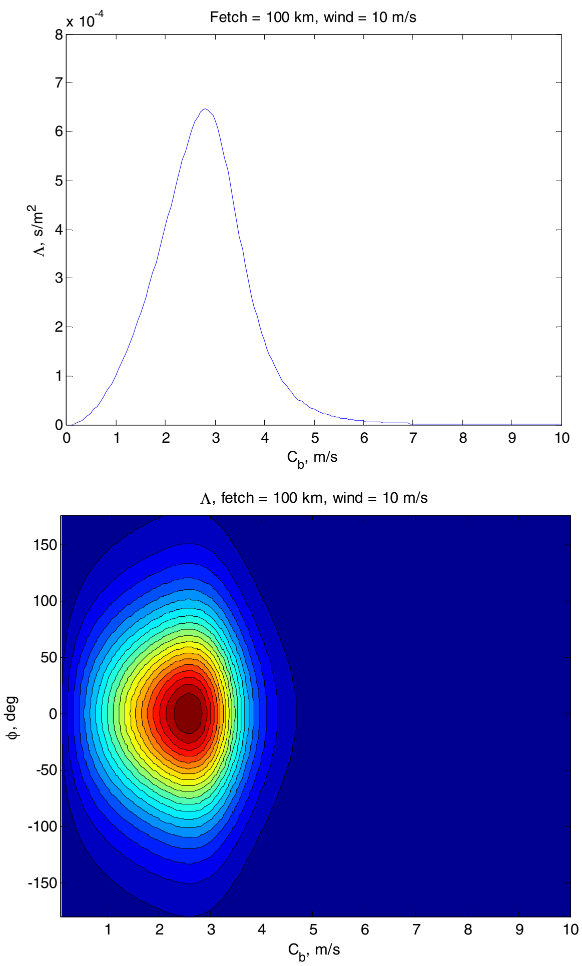


Figure 1. The form of $\Lambda(\mathbf{c_b})$ derived from the DBP Spectrum of Plant [6] at a fetch of 100 km and a wind speed of 10 m/s. Top = $\Lambda(\mathbf{c_b})$ integrated over azimuth angles. Bottom = $\Lambda(\mathbf{c_b})$ dependence on $c_b$ and azimuth angle, $\phi$.

## III. MODELING BREAKING WAVE EFFECTS ON MICROWAVE BRIGHTNESS TEMPERATURE

We used this form of $\Lambda(\mathbf{c_b})$ to include foam effects in the radiometer model. Foam coverage is calculated from the equation

$$f = a\int c_b^3\,\Lambda(c_b)dc_b$$

with $a = 0.3\ \mathrm{s^3m^{-2}}$. This equation has been derived by assuming that the lifetime of foam on the sea surface is proportional to $c_b^2$. Figure 3 shows our calculated foam coverage for various fetches compared with measurements by Monahan (1971) [7].

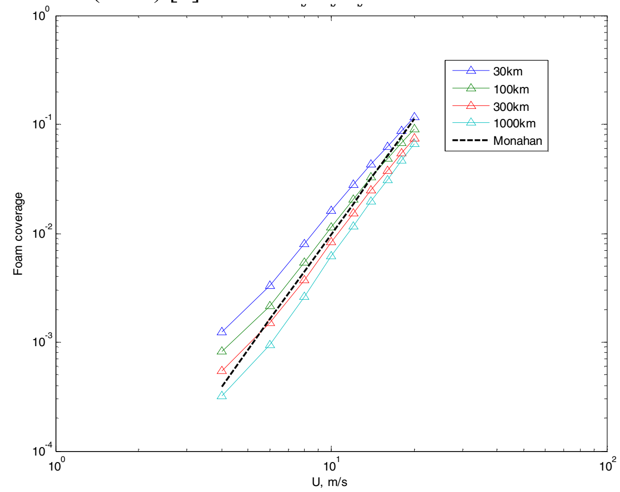


Figure 2. Foam coverage versus wind speed from our model and from the measurements of Monahan [7].

Having this estimate of coverage, we treated sea foam as a structure with multiple horizontal layers and a dielectric constant smoothly changing from 1 to that of sea water with increasing depth. Following Anguelova [8] we assume exponential vertical distribution of the void fraction and use the Polder-vanStanten mixing formula to get the effective dielectric constant of a sublayer. Reflection and emission of microwaves are calculated by solving the multiple reflection problem. Calculation of the brightness temperature contrast due to wave breaking includes averaging over foam lifetime, averaging over multiple breakers (Λ-function), and averaging over local slopes. Effects of non-breaking sea waves on the brightness temperature are included using the model spectrum that yielded $\Lambda(\mathbf{c_b})$ and the small-slope approximation [9].

Figure 4 shows an example of the output of this model compared with the empirical model from Meissner and Wentz [10] for 6.8 GHz and 52 degree incidence angle. Meissner and Wentz derived approximating functions summarizing the bulk of WindSat data. Our radiometric model accounts for non-breaking waves and foam produced by breakers. So far, the model does not account for steep and bound waves associated with breaking but it appears to predict the correct wind speed dependence at vertical and horizontal polarizations.

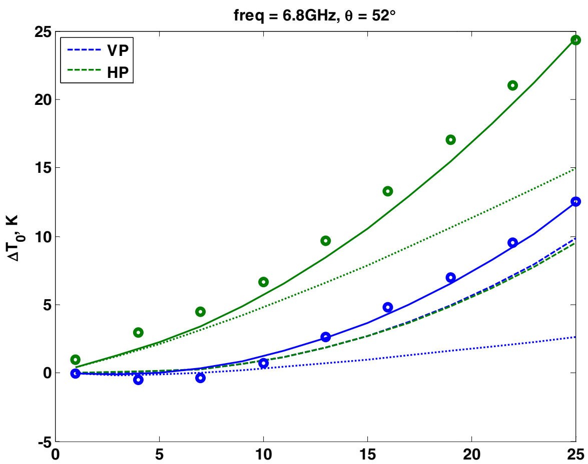

Figure 4. Circles show the empirical model functions derived by Meissner and Wentz [10] for WindSat. Dotted lines show the effect of sea waves calculated by small-slope approximation and dashed lines show the brightness temperature increase due to the foam. Solid lines are the sums of the roughness and foam contributions. Blue lines and symbols correspond to vertical polarization and the green ones to horizontal polarization. Azimuthally averaged brightness temperature contrasts are shown.

## IV. MODELING MICROWAVE BACKSCATTER FROM FREE, BOUND, AND BREAKING WAVES

We modified the multiscale model of Plant [6] to includes both the roughness due to gently breaking waves (bound waves) and the surface deformations produced by more strongly breaking waves (breaking waves) in addition to the freely propagating wind-generated waves postulated by the original model (free waves). We envision all scatterers as being small or intermediate-scale waves in the sense described by Plant [6] so that they are tilted and advected by longer waves. Then the total normalized radar cross section of the sea due to all these processes be given by

$$\sigma_o = P_f\, \sigma_o^f + P_b(\sigma_o^b + \sigma_o^{br})$$

where "f" indicates free waves, "b" indicates gently breaking or bound waves, and "br" indicates more strongly breaking waves, $P_f$ is the probability of finding free waves and $P_b$ is the probability of finding bound or breaking waves. Furthermore, we assume that bound and breaking waves do not occur at the same time and place as free waves due to the suppression of the free waves in regions of turbulence produced by breaking waves. Thus the probability distributions of long-wave slopes are different for bound/breaking waves and free waves but are the same for gently and strongly breaking waves since both types of breaker are produced in a breaking zone. Note that these assumptions imply that

$$P_f + P_b = 1$$

We used values of $P_f$ and $P_f$ versus wind speed that were obtained by Plant [11] by fitting Gaussian probability distribution functions for both free and bound waves to the data of Cox and Munk [12].

The primary difference between free and bound waves is that the probability distribution of bound waves is shifted toward the downwind face of the long waves so the mean slope of bound waves is negative. This implies that to maintain a zero slope for the overall sea surface, the free waves must have a positive mean slope. We added bound waves to the original multiscale model by letting $\sigma_o^f$ be those given by the original model but shifting their probability distribution to a small positive slope and calculating $\sigma_o^b$ from

$$\sigma_o^b = 8\pi k_o^4 \int |g_{pp}^{'}|^2 P(s|bx)\psi_b\, ds$$

where $k_o$ is the microwave length, $g_{pp}^{'}$ is the geometric factor given by Plant [6] for polarization p, $P(s|bx)$ is the probability distribution of slopes given that the waves are bound waves, and $\psi_b$ is the bound wave spectral density. We let this be equal to 1.8 $\psi_m$, the spectral density of the model spectrum. The sum of sum of free and bound waves weighted by their probabilities must be the model spectrum:

$$P_f\psi_f + P_b\psi_b = \psi_m$$

We did not attempt to model the exact shape of the breaking waves but assumed a collection of tilted dihedrals of the type shown in Figure 4.

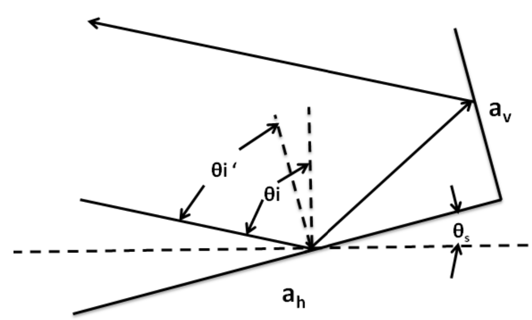


Figure 4. Diagram of a tilted dihedral.

Plant et al. (2010) postulated that the cross section of such dihedrals is given by

$$\sigma = A_p|R_2|^2 D$$

where

$$A_p = w(a_v \cos\theta_i^{'} + a_h \sin\theta_i^{'})$$

$$R_2 = \left[R_v(\theta_i^{'})\exp\left(-\frac{i\pi}{2}\right)\cos\varphi + R_h(\theta_i^{'})\sin\varphi\right]\left[R_v\left(\frac{\pi}{2} - \theta_i^{'}\right)\exp\left(-\frac{i\pi}{2}\right)\cos\varphi + R_h\left(\frac{\pi}{2} - \theta_i^{'}\right)\sin\varphi\right]$$

$$D = k_o^2 A_p/\pi$$

where w is the crest length of the dihedral (perpendicular to the page), φ is the angle of the electric field with respect to the plane of incidence, $R_v$ and $R_h$ are Fresnel reflection coefficients for vertical and horizontal polarization, respectively, and the other symbols are defined in Figure 4.

Following Duncan's measurements of the height of the toe of the breaker [13] , we let

$$a_v = \alpha\lambda = \frac{2\pi\alpha}{k}.$$

Where λ is water wavelength, k is wavenumber, and α is a constant between 0.002 and 0.003. Note that this implies that the present model is not valid if λ is less than a few meters long since in that case, $a_v$ would be less than the microwave length and physical optics would not apply. Disturbances produced by such short waves can be considered bound waves. We then assume that $a_h$ is not fixed but given by

$$a_h = a_v \tan\theta_i^{'}.$$

Phillips [2] shows that the average width w of a breaking wave is inversely proportional to k. Calling the constant of proportionality 1/β, we have for the mean normalized radar cross section of breaking waves,

$$\sigma_o^{br} = 16\pi k_0^2 \left(\frac{\alpha}{\beta}\right)^2 D(\phi) e^{-4k_0^2\alpha_b^2\cos^2\theta_i} \cdot \int |R|^2 \sin^2\theta_i^{'} P(\tan\theta_s|b)d\theta_s \int k^{-3}\Lambda(k)dk.$$

Where the exponential factor accounts for bound waves that exist on the horizontal plane of the dihedral.

Figure 5 shows the result of computing $\sigma_o$ as a function of incidence angle using these equations at a wind speed of 8 m/s for upwind, crosswind, and downwind azimuthal look directions. We let α = 0.003 and β = 12 in these calculations. The data points shown in this figure are those also shown in Figure 8 of Plant et al. [13].

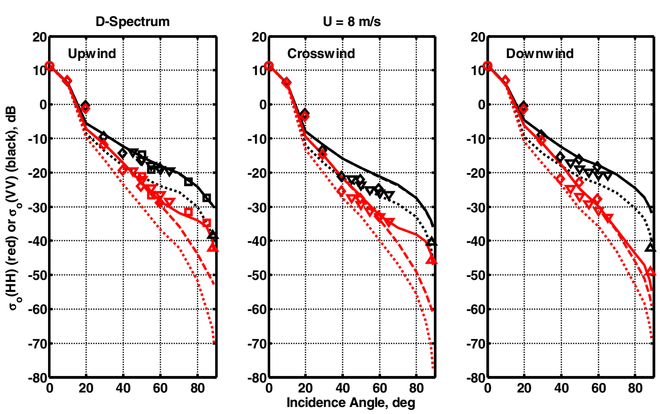


Figure 5. Calculated $\sigma_o$ values for the DBP spectrum of Plant 2002. Dotted lines = no bound or breaking waves, dashed lines = no breaking waves, solid lines = full model.

## IV. CONCLUSION

We have developed a joint active/passive model of the microwave signatures of the sea surface. The model uses a single directional wave spectrum as input and yields estimates of microwave brightness temperatures and normalized radar cross sections of the sea. Past models have been improved by including bound and breaking waves. Bound waves increase the normalized radar cross section at incidence angles greater than about 45°. Breaking waves produce foam which is an important source of brightness temperature and also increase backscatter at HH polarization at incidence angles above about 60°. The model has been tested here at C, X, and Ku bands. Tests at other frequencies will be conducted in the near future.

## ACKNOWLEDGMENT

This work was supported by the NASA Remote Sensing Theory Program, Grant # NNX11AL27G.

## REFERENCES

[1] Wright, J. W.: 1968, 'A New Model for Sea Clutter', IEEE Trans. AP-16, 217-223.

[2] Phillips, O. M. (1985), Spectral and statistical properties of the equilibrium range in wind-generated gravity waves, J. Fluid Mech., 156, 505–531, doi:10.1017/S0022112085002221.

[3] Plant, W.J., 1997: A model for microwave Doppler sea return at high incidence angles: Bragg scattering from bound, tilted waves, J. Geophys. Res, 102(C9), 21131-21146.

[4] Plant, W.J., 2012, Whitecaps in deep water, Geophys. Res. Ltrs., 39, L16601, doi:10.1029/2012GL052732.

[5] Banner, M. L. and R. P. Morison, 2010: Refined source terms in wind wave models with explicit wave breaking prediction. Part I: Model framework and validation against field data. *Ocean Modell., 33,* 177–189.

[6] Plant, W.J., 2002, A stochastic, multiscale model of microwave backscatter from the ocean, J. Geophys. Res.,107(C9), 3120, doi:10.1029/2001JC000909.

[7] Monihan, E.C., Oceanic Whitecaps, 1971, J. Phys. Ocean., 1, 139-144.

[8] Anguelova, M.D., 2008, Complex dielectric constant of sea foam at microwave frequencies, J. Geophys. Res., 113(C8), doi: 10.1029/2007JC004212.

[9] Irisov, V.G., Azimuthal variations of the microwave radiation from a slightly non-Gaussian sea surface, Radio Sci., 35(1), 65-82, 2000..

[10] Meissner and Wentz, 2012, The Emissivity of the Ocean Surface Between 6 and 90 GHz Over a Large Range of Wind Speeds and Earth Incidence Angles , 50(8), TGRS, 3004-3026

[11] Plant, W.J., 2003: A new interpretation of sea-surface slope probability density functions, J. Geophys. Res, 108(C9), 3295, doi:10.1029/2003JC001870.

[12] Cox, C. and W. Munk, Statistics of the sea surface derived from sun glitter, J. Mar. Res., 13(2), 199-227, 1954.

[13] Duncan, J. H., 1981: An experimental investigation of breaking waves produced by a towed hydrofoil. *Proc. Roy. Soc. London, 377A,* 331–348.

[14] Plant, W. J., W. C. Keller, K. Hayes, and G. Chatham, Normalized radar cross section of the sea for backscatter, 2010: 1. Mean levels, J. Geophys. Res., 115, C09032, doi:10.1029/2009JC006078.